Natural Hazards **9**: 215–233, 1994.

Seismic Hazard Analysis with Randomly Located Sources

M. SEMIH YUCEMEN and POLAT GULKAN
Department of Civil Engineering and Earthquake Engineering Research Center, Middle East Technical University, 06531 Ankara, Turkey

(Received: 3 December 1991; in final form: 30 March 1993)

Abstract. Demarcation of areal and linear seismic sources involves a certain degree of uncertainty and this should be reflected in the final seismic hazard results. The uncertainty associated with the description of the geographical coordinates of a source zone boundary is modeled by introducing the concept of 'random boundary', where the location of the boundary is assumed to exhibit a spatial bivariate Gaussian distribution. Here the mean vector denotes the best estimate of location and the variance reflects the magnitude of location uncertainty, which may be isotropic or may show spatial directivity. The consideration of spatial randomness in the boundaries smooths the seismicity parameters and permits the gradual transitions of these to occur across border zones. Seismic sources modeled as lines can also be attributed random geometrical properties.

The sensitivity of seismic hazard results to the isotropic and direction dependent location uncertainty is examined on the basis of hypothetical case studies. Area and line source location uncertainties are examined separately because they are reflected in the eventual outcome of the analyses in a complicated manner. The effect of random source zone boundaries on the expected peak ground acceleration is tested for a specific site in Turkey by conducting a comprehensive seismic hazard analysis.

Key words: Seismic hazard, random source location, random boundary, source zone boundary, seismic sources, uncertainty, earthquakes, statistical analysis.

1. Introduction

Virtually every region in the world is under the threat of some form of natural hazard, and each year the occurrence of disasters causes much loss of life and property. The vulnerability to natural disasters of human populations and settlements can be reduced by a multidisciplinary approach where the physical hardening of engineered facilities is one component. Other means of reducing potential losses include prediction or forecasting and preparedness, both for the pre- and post-disaster phases (U.S. National Committee for the Decade for Natural Disaster Reduction, 1991).

Rational engineering design against effects engendered by natural hazards requires that those effects be identified and quantified. Past practice for the assessment of hazard was generally carried out from a deterministic point of view, in which the uncertainties associated with various hazard parameters are not treated explicitly, however, to compensate for these uncertainties, conservative values are

assumed for them. Considering the randomness in the occurrence of natural hazards with respect to time, space and magnitude and the various sources of uncertainties a probabilistic approach appears to be more appropriate. As a result, probabilistic procedures have in the last two decades become the subject of growing interest and demand for evaluating the environmental hazards at a specific site as well as developing hazard maps which portray their geographical distribution.

In probabilistic seismic hazard analysis the hazard parameters are taken as random variables, and are described by probability distributions. Besides this randomness one has to consider the uncertainties associated with the assumed relationships and input models. An important source of uncertainty is associated with the geographical coordinates describing potential sources from which natural hazard nucleates. In this study, the problem of identifying hazard sources in space and modeling the location uncertainty are addressed considering only the seismic hazard. However, it is believed that the methodology presented herein is general and applicable to other types of natural hazards with slight conceptual modifications.

The spatial distribution of earthquakes is described by associating them with seismic sources which are generally modeled either as lines or areas. In the demarcation of potential seismic sources, geotechnical, seismological and tectonic information must be taken into consideration.

If the earthquake epicenters within a region fall along a major fault system, a line source, with a uniform probability of occurrence along its length may be used to model the location of future epicenters (or hypocenters). In some regions it may not be possible to correlate the past seismic activity with any of the existing geologic structures or it may not be possible to identify the geologic structures due to deep overburdens. In such regions it is assumed that earthquakes are equally likely to nucleate anywhere and they are treated as area sources. This has lead to the concept of seismotectonic provinces which are modeled either as area sources, or as areal entities containing well-defined fault structures.

The description of the spatial configuration of potential seismic sources is quite a difficult undertaking, and requires the consideration of many variables. In practice one must be guided by tectonic maps and epicenter maps. The final decision on how to model the geometry of seismic sources relies largely on expert opinion and thus on personal judgment.

The basic of aim of this study is to model the uncertainty in the location of earthquake source coordinates and to evaluate its consequences for hazard analysis. This is achieved by assuming the source zone coordinates to be 'random' rather than deterministic. The physical treatment of the uncertainty in the boundaries of an area source is different from that concerning the uncertainty in the precise orientation of a fault zone and its length. The numerical exercises devised in the next section treat these two categories separately because it is difficult to quantify the way each perturbation is ultimately absorbed into the final outcome which is the expected ground acceleration along a string of points.

This paper demarcates areas of different seismic hazard on the basis of calculated ground acceleration values. Implicitly these acceleration peaks are assumed not to be influenced by local geological conditions. There is of course ample evidence that these conditions play just as important a role in the forces which influence built facilities during earthquakes, but this is an issue which lies totally outside our scope.

In its current format the paper addresses the question: how can areas with different seismic hazard potential be more reliably differentiated? The ultimate beneficiary of the answer to this question might be an emergency planner or a code official. What such groups require is a means of drawing a multi-colored map identifying the hazard zones definitions only. The index which assigns a particular color to a particular point will be taken as the expected ground acceleration at that point. In theory, other indices (intensity, velocity or displacement) could also have been used as the yardstick, but the acceleration is chosen because of its relative convenience. We note that in more or less concealed fashion, the ground acceleration value is the basis of design requirements in many codes.

2. Modeling Seismic Zone Location Uncertainty

Delineation of seismic sources based only on the spatial distribution of past seismic activity may lead to serious errors. The assumption of sharp boundaries among area sources or fixed (deterministic) locations for line sources introduces an artificial bias in the seismic hazard values. In the classical seismic hazard analysis model (e.g. McGuire, 1976) the uncertainty in the shape and location of earthquake sources is ignored, and the resulting errors are not reflected in the final results. This is due mainly to the fact that the computations are performed according to an algorithm in which the zone boundary location uncertainty is not a parameter. This difficulty is generally bypassed by carrying out sensitivity analyses and by computing a mean hazard curve averaged over the hazard results corresponding to alternative source configurations. These alternatives can be presented also in a logic tree format. The weights are assigned subjectively and the averaging is done by using the discrete form of the theorem of total probability.

In this study, a model proposed by Bender (1986) is refined by assuming a direction dependent randomness in the spatial coordinates of seismic sources in order to incorporate the uncertainty in their location directly. The types of seismic sources considered include both areas and lines. In Bender's model the mean locations of earthquakes in an earthquake source are uniformly distributed, but the scatter around each mean is a bivariate 'circular' normal distribution. Here, this will be referred to as the 'isotropic' uncertainty case where, if σ is the standard deviation in the expected coordinates $(\bar{x}, \bar{y})$ of an earthquake inside a source, then the probability that the earthquake will migrate by (δ_x, δ_y) is proportional to the density function:

$$f(\delta_x, \delta_y) = \frac{1}{2\pi\sigma^2} \exp\left(- \frac{\delta^2{}_x + \delta^2{}_y}{2\sigma^2} \right) \tag{1}$$

If the location uncertainty for a given point is unequal in two orthogonal directions, then Equation (1) must be modified:

$$f(\delta_x, \delta_y) = \frac{1}{2\pi\sigma_x\sigma_y} \exp\left[- \left(\frac{\delta_x^2}{2\sigma_x^2} + \frac{\delta_y^2}{2\sigma_y^2} \right) \right] \tag{2}$$

This will be referred to as the 'biased' uncertainty case where an earthquake may occur inside an oval area surrounding its expected location. The uncertainty in the boundary of a given source can be reflected on the ground motion parameter (commonly the ground acceleration) at the site on the basis of the following argument: When earthquakes inside a given source are shifted by (δ_x, δ_y) from their expected location, this in effect defines a source zone shifted by the same amount. The possible location of a source zone, and not necessarily the coordinates of the earthquakes occurring inside it, is regarded as normally distributed, so the probability density function of the source zone being relocated by (δ_x, δ_y) is given by Equation 2. The ground motion parameter rate at the point of interest may therefore be computed as the weighted average of the rates of the parameter in the same interval calculated for a fixed source location with uniform seismicity (Bender and Perkins, 1987). In effect, then, the calculation of the weighted average for the ground motion parameter is a smoothing process where the multipliers are the ordinates of the expression in Equation 2. Also, as the boundaries of the source zones become increasingly more random, the extent of the area which will be affected becomes stretched in both directions.

In the case of faults, which are idealized as line sources, the location uncertainty is attributable to two causes: the precise location of the fault line and the fault rupture length. Accordingly the randomness in the location of a fault is restricted to two orthogonal directions. These directions are selected as normal to the fault line and along the fault line. In the direction normal to the fault line the location uncertainty is denoted by Δ_f. The possible locations of the fault is now obtained by shifting the fault parallel to its mean location in both directions. The shift distance is assumed to be uniformly distributed over a range of $\pm\frac{1}{2}\Delta_f$.

The location uncertainty along the axis of the fault is reflected in the hazard analysis through a randomness introduced between rupture length and magnitude, where a log-linear relation is known to exist between fault rupture length and magnitude (Slemmons, 1977). In the model for a given magnitude the rupture length is assumed to be lognormally distributed with a standard deviation denoted by δ_l. This way the rupture length is permitted to extend in a random way beyond the median length at the end points, and is proportional to σ_l. Here σ_l is the

standard deviation of $\log(l)$ and is approximately equal to the coefficient of variation of l.

3. Numerical Experiments

Standard methods of probabilistic seismic hazard analysis require an occurrence model, a probability distribution for magnitudes, an attenuation relationship and spatial distribution of seismic zones. The resulting hazard function generally gives the annual probability of a specific ground motion parameter being exceeded. A detailed derivation of the hazard function is given in Gulkan and Yucemen (1977).

In the following, three different numerical experiments will be performed to examine systematically the sensitivity of seismic hazard results to different values of earthquake location uncertainty in two perpendicular directions. These results can be considered as a sequel to a recent study by Gulkan and Yucemen (1991), in which the only type of seismic zone considered was the area (Bender and Perkins, 1987).

The only deviation in the following examples from the 'classical' seismic hazard analysis (e.g. McGuire, 1976) is the incorporation of uncertainty into the zone boundary locations in an explicit way. As such, it requires the specification of the standard deviation of the epicentral locations of earthquakes associated with a particular region. The first two examples are necessarily abstract, because they refer to a highly idealized two-source region and are concerned only with highlighting the effect of impaired knowledge of zone boundary location on the calculated expected acceleration values along profiles bisecting the zones in meridional or transverse directions. The third example draws from an actual case study; there is nothing special about this region other than the fact that its seismicity parameters were available from a previous study (Doyuran *et al.*, 1989).

3.1. *Experiment No. 1*

In this hypothetical problem two area sources, shown in Figure 1a, are considered. Zone 1 is assumed to experience ten times more seismic activity per unit time than does Zone 2. The felt region under consideration is 4 degrees wide by 2 degrees high rectangle. This represents an area of approximately 350 km by 220 km. The acceleration levels corresponding to a 0.90 probability of not being exceeded during 100 years are calculated across two E-W and N-S profiles considering five combinations of the uncertainty in the source boundaries. The profiles are shown in Figure 1a and with x and y representing the E-W and N-S directions, respectively, these five combinations are given by the following five cases:

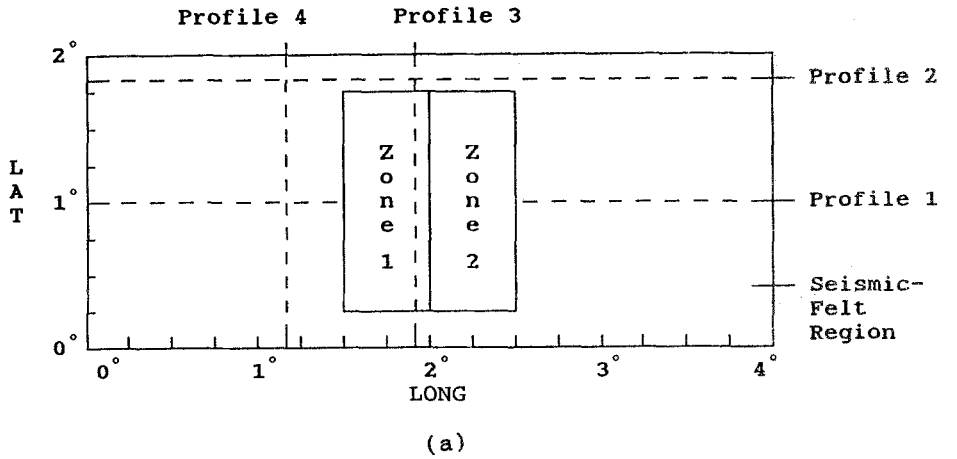

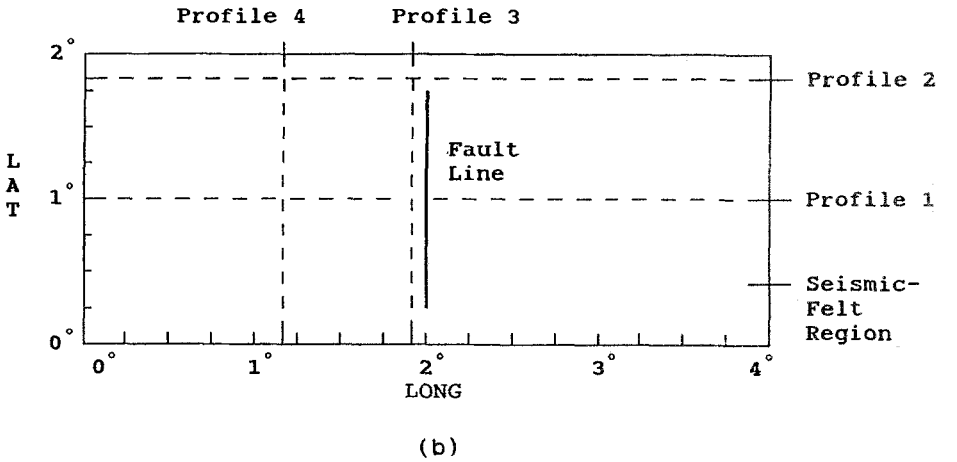

Fig. 1. Hypothetical study areas: (a) Experiment No. 1; (b) Experiment No. 2.

Case 1	Case 2	Case 3	Case 4	Case 5
$\sigma_x = 0$ km	$\sigma_x = 12$ km	$\sigma_x = 24$ km	$\sigma_x = 0$ km	$\sigma_x = 12$ km
$\sigma_y = 0$ km	$\sigma_y = 12$ km	$\sigma_y = 24$ km	$\sigma_y = 12$ km	$\sigma_y = 0$ km

The hazard curves are placed in two groups. In the first, the isotropic uncertainties (Cases 1–3) are compared with one another and in the second the biased cases (Cases 4 and 5) are compared with Case 2.

The abrupt change of expected seismicity at source boundaries of Figure 2a is

immediately dispelled when the location uncertainty is introduced. It is to be noted that with increasing σ, transition becomes smoother, but the expected ground acceleration value within the zones remains at a comparable level. Profile 1, which traverses the study area centrally appears to be nominally affected by biased uncertainty, shown in Figure 2b. This effect is more pronounced for Profile 2 which is just to the north of both source zones. In Figure 3a it is observed that a significant increase occurs in the ground acceleration as soon as σ in both principal directions is introduced. In Figure 3b it is seen that it is σ_y which controls the seismicity of this profile: Cases 2 and 4 differ only in the way they blend in from areas not contiguous to the source zones to the northern projections of both sources, while the expected maximum is about the same. The conclusion is, if any uncertainty exists in the northern boundary of the source zone a corresponding large increase occurs in the hazard level.

In plotting the hazard curves along Profiles 3 and 4 the acceleration and distance axes are interchanged. In contrast to Figures 2 and 3, Figures 4 and 5 show expected ground acceleration on the horizontal axis, and the distance expressed as degrees latitude on the vertical axis.

For profiles 3 and 4 the influence of random borders is presented in Figures 4 and 5, respectively. Note that apart from a more gradual transition of the lines for Profile 3, which traverses the study area by passing through Zone 1, σ has a relatively minor influence on the acceleration level. As soon as one steps outside the source areas, however, major differences may be calculated, depending on how close the chosen value of σ_x effectively brings the source boundary close to the profile (Figure 4). In Figure 5b the closeness of Cases 2 and 5 proves that σ_y has a minor role in determining the increases of expected seismicity depicted in Figure 5a.

3.2. *Experiment No. 2*

In this problem again the same region is considered but the two area sources are now replaced by a single fault extending in the N-S direction as shown in Figure 1b. The acceleration levels corresponding to a 0.90 probability of not being exceeded during 100 years are calculated across the same four profiles considering five combinations of Δ_f and σ_l. Here, Δ_f describes the uncertainty in the location of the fault in a direction perpendicular to the axis of the fault (i.e. in E-W direction) and σ_l denotes the uncertainty in the extension of the end points of the fault in the N-S direction due to random variations in the rupture mechanism. These five combinations form Cases 6 to 10 as described below:

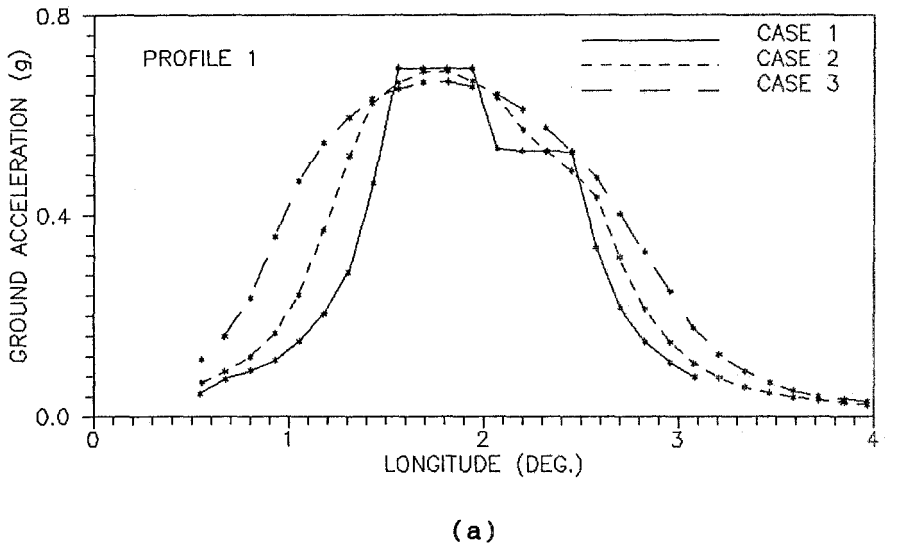

(a)

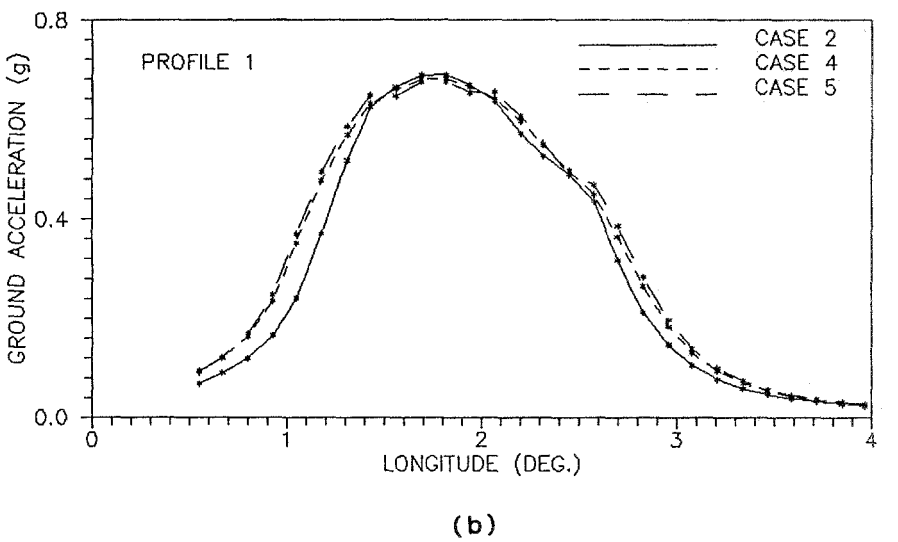

(b)

Fig. 2. Hazard calculated for Profile 1 (Experiment No. 1).

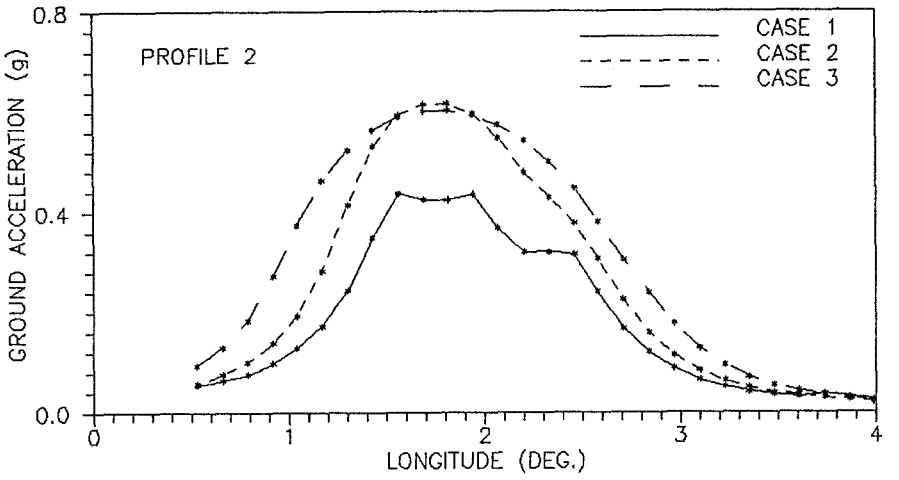

(a)

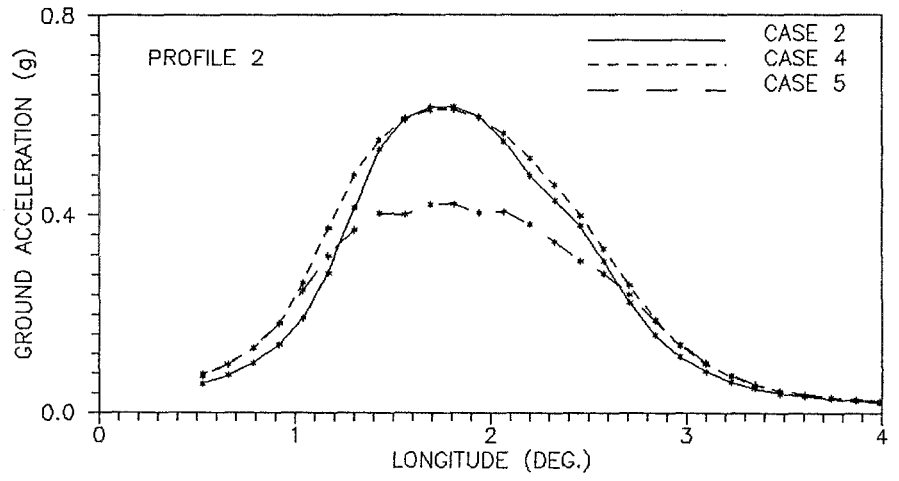

(b)

Fig. 3. Hazard calculated for Profile 2 (Experiment No. 1).

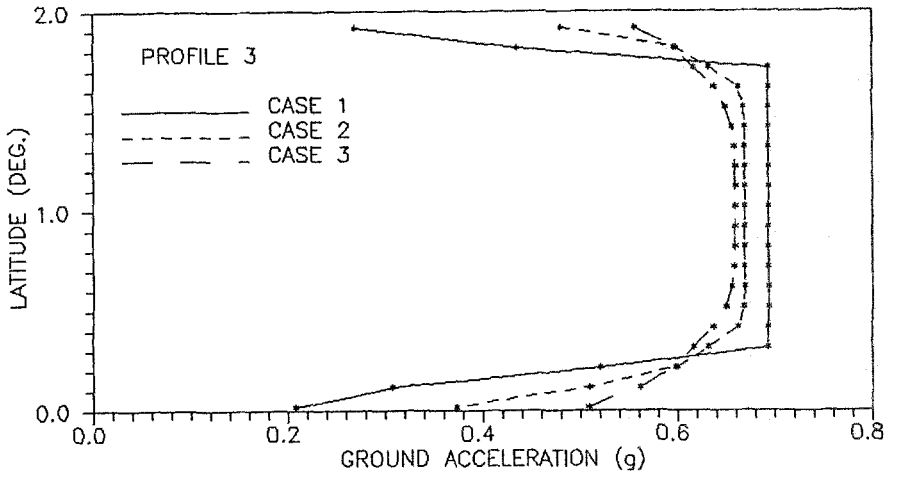

(a)

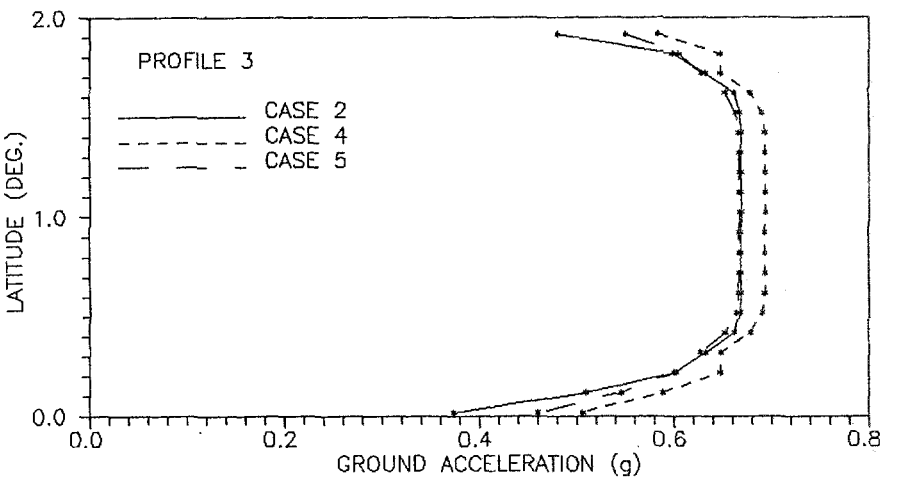

(b)

Fig. 4. Hazard calculated for Profile 3 (Experiment No. 1).

Case 6	Case 7	Case 8	Case 9	Case 10
$\Delta_f = 0$ km	$\Delta_f = 12$ km	$\Delta_f = 24$ km	$\Delta_f = 12$ km	$\Delta_f = 12$ km
$\sigma_l = 0.5$	$\sigma_l = 0.5$	$\sigma_l = 0.5$	$\sigma_l = 0$	$\sigma_l = 1.0$

The rate of seismic activity for the fault has been artificially calibrated to be

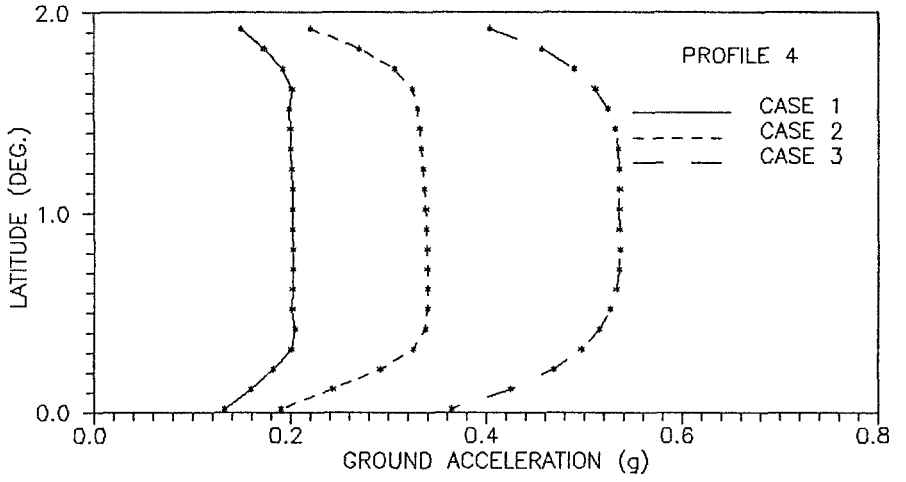

(a)

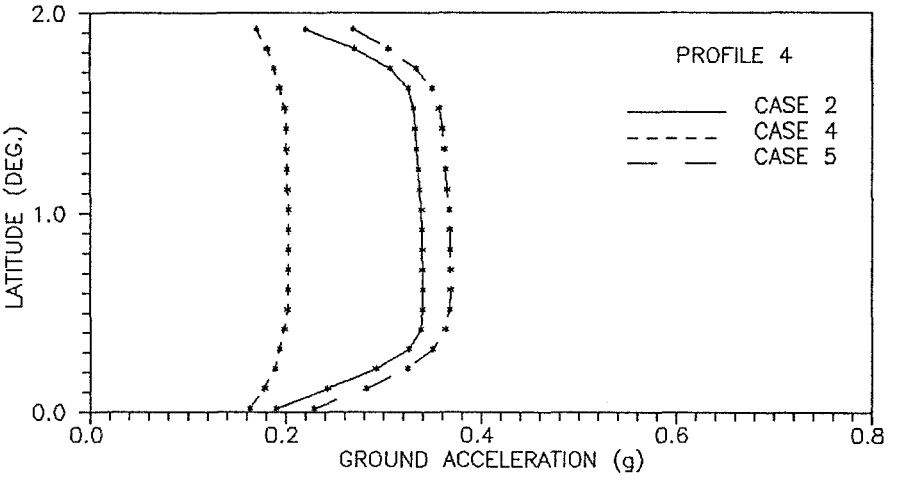

(b)

Fig. 5. Hazard calculated for Profile 4 (Experiment No. 1).

comparable to that of Zone 1 of the first Experiment, but apart from this property all of the items which contribute to the final numerical output are completely fictitious. We therefore refrain from making any comments on the hazard ordinates.

Hazard curves calculated for Profile 1 are grouped in the frames of Figure 6. When the N-S fault line occupies a zone of increasing thickness there appears to be an increase in the magnitude of the estimated hazard, but whether the zone is 12 km or 24 km is immaterial as seen in Figure 6a. Part (b) of the same figure is self-evident because variation in the length of the fault zone would be expected to play a major role only near the tips, and not along Profile 1 which is equator-like for the felt area. The exact shape of the hazard curve is of course a function of the attenuation relation used in calculating the hazard ordinates, but for the type of abatement of ground acceleration over distance which was used in the study the overall shapes of the hazard curves centered on the fault zone are in conformance with expectations. It is to be noted that increasing the degree of diffuseness of the fault also broadens the width of the region which will be subjected to a given ground acceleration.

Figure 7 exhibits a contrasting tendency of calculated hazard when the uncertainty is associated with the length of the fault. Note that the width of the fault line plays no role on hazard (Figure 7a) while its length does, (Figure 7b).

The information conveyed by Figure 8a is essentially the same as that contained in Figure 6a: When the fault is synonymous with the meridian centered at 2 degrees, there exists constant acceleration hazard along it. (Note that the fault is described as having a length of 1.5 degrees.) With increased width of the area within which the fault may lie, the expected hazard also increases, but remains constant along the fault. As would be anticipated, the variation of the length of the fault plays a role only near the extremities of the fault, which may reach large differences over relatively short distances, as shown in Figure 8b.

Frames (a) and (b) of Figure 9 confirm that at distances away from seismic sources, the calculated hazard shows trivial variations due to migration of earthquakes associated with them, except possibly at points across the tip of the fault lines. The general level of hazard in the two frames of this figure is of small magnitude, and could be linked with greater sensitivity to the attenuation function.

3.3. *Experiment No. 3*

A particular construction site on the south coast of Turkey is considered as the third numerical Experiment. A number of seismic source configurations, exhibiting significant differences were proposed for the site over the last 16 years (Doyuran *et al.*, 1989, Gulkan and Yucemen, 1977). The most recent proposal is shown in Figure 10. Note that no line source is identified over the region.

The sensitivity of seismic hazard results to location uncertainty is tested for the site shown in Figure 10 within source zone R11. The input data are taken directly

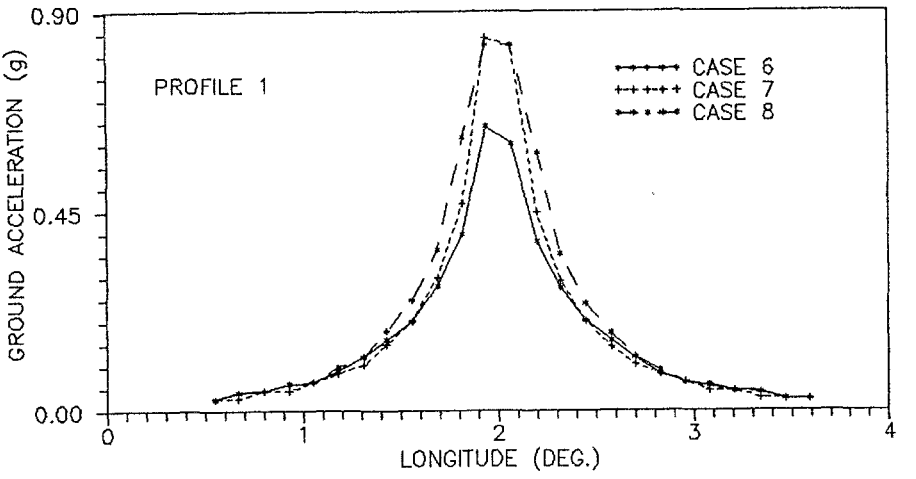

(a)

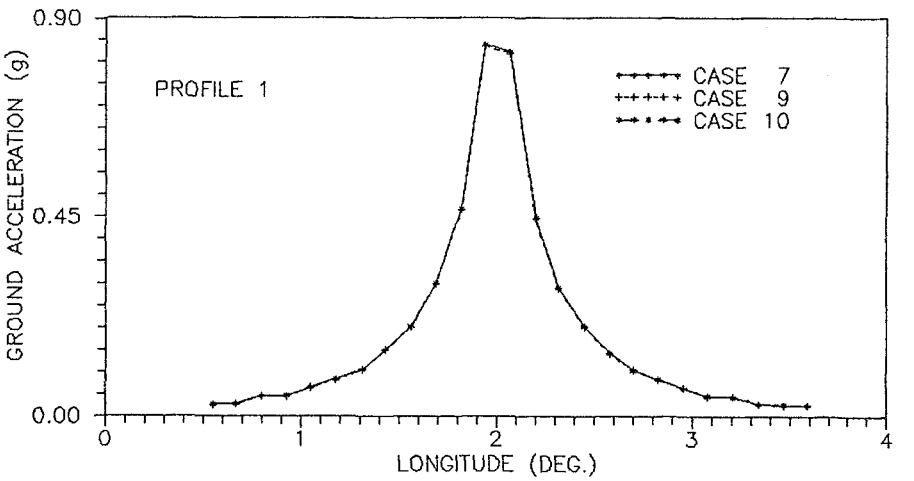

(b)

Fig. 6. Hazard calculated for Profile 1 (Experiment No. 2).

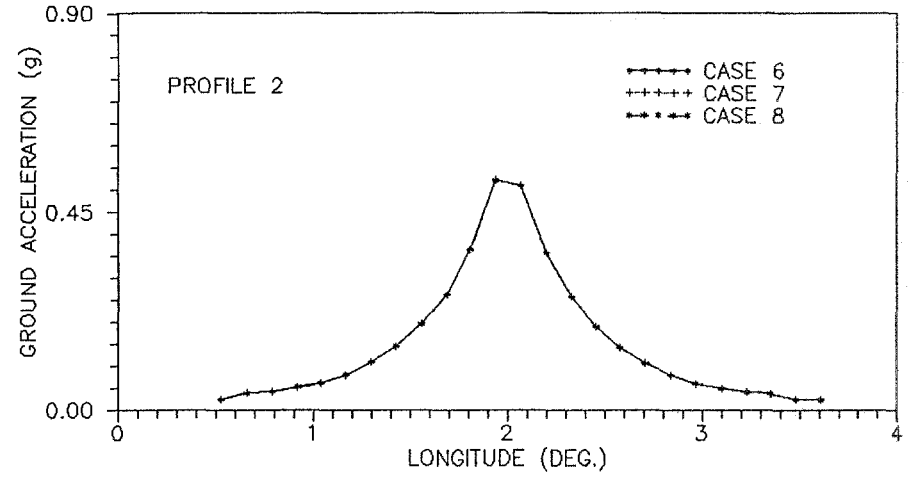

(a)

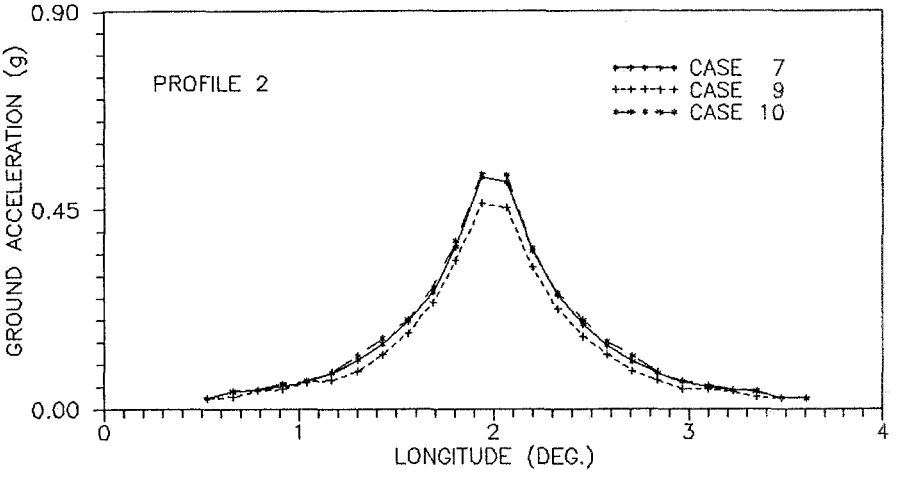

(b)

Fig. 7. Hazard calculated for Profile 2 (Experiment No. 2).

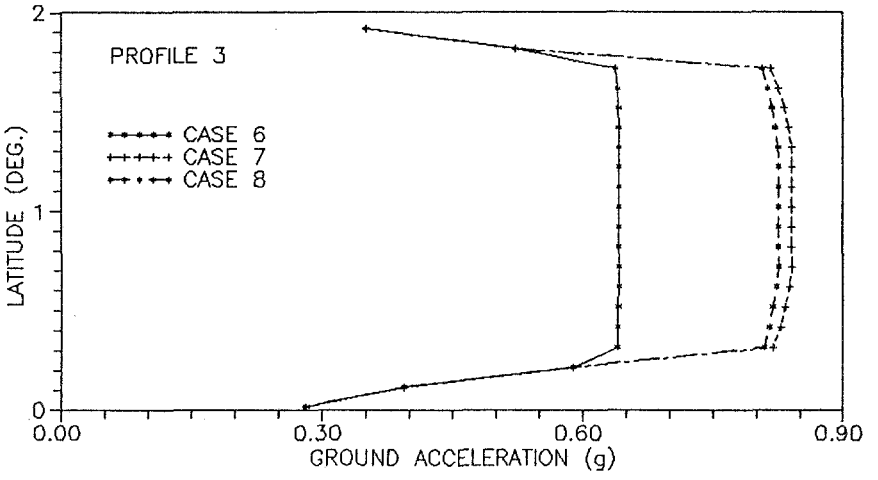

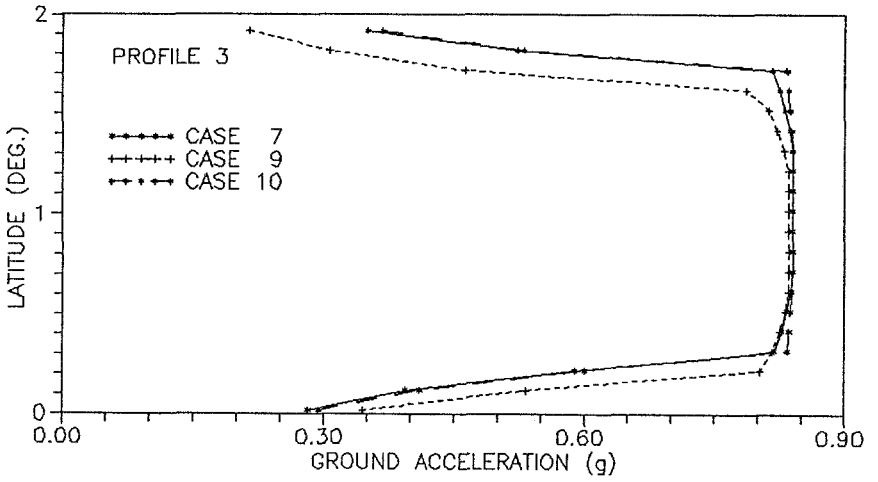

Fig. 8. Hazard calculated for Profile 3 (Experiment No. 2).

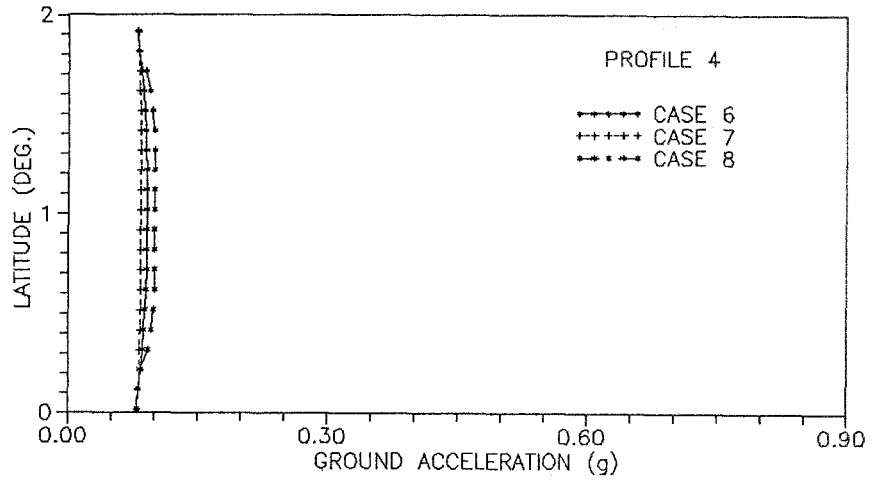

(a)

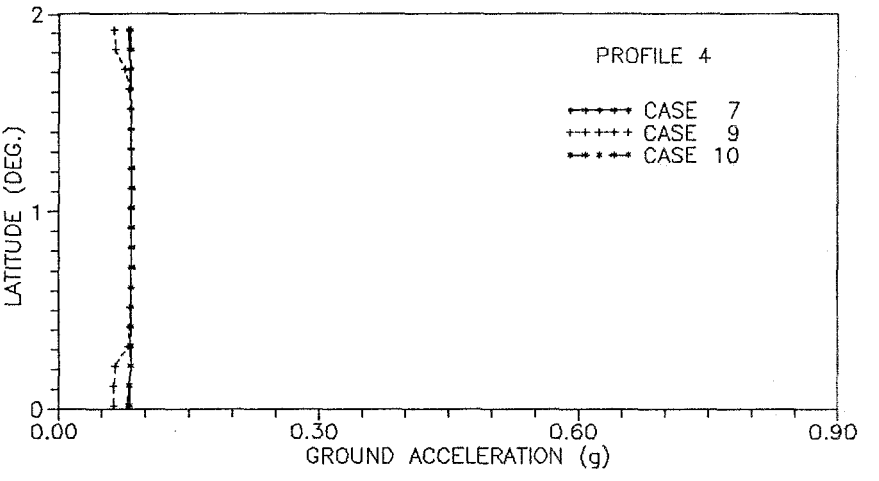

(b)

Fig. 9. Hazard calculated for Profile 4 (Experiment No. 2).

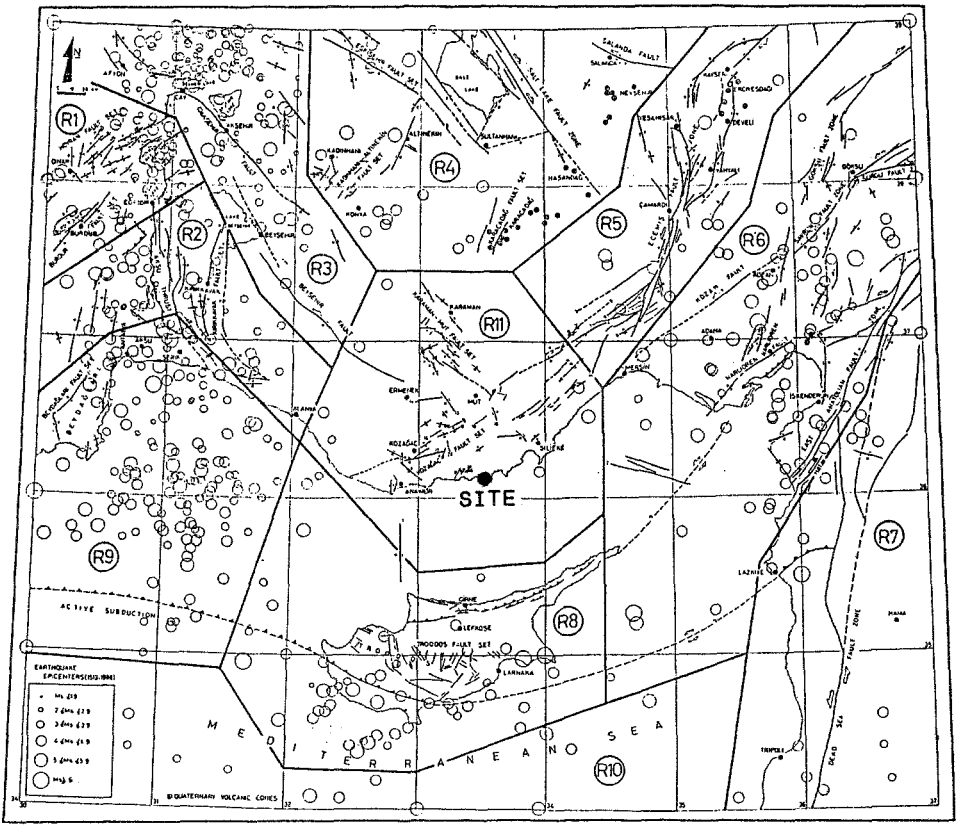

Fig. 10. Seismic source zones used in Experiment No. 3 and the location of the site.

from Doyuran *et al.* (1989). The hazard function corresponding to five cases (Cases 1–5) of zone boundary uncertainty are computed and the corresponding hazard curves are shown in Figure 11. In order to carry out the comparison at small risk levels a very long return period of 100 000 years is considered. As seen in Figure 11a, an increase in σ_x or σ_y causes a corresponding increase in the hazard, expressed by a shorter return period for the same ground acceleration. On the other hand, as Figure 11b indicates, a biased variation of boundary location is not meaningful when the point of interest is situated far from the boundaries. As corollary to this observation we may also speculate that points lying in the vicinity of source boundaries will show noticeable variations in hazard studies.

4. Conclusions

In this study the uncertainty associated with the demarcation of seismic source zones has been considered explicitly in the calculations of hazard. This is achieved by treating the spatial coordinates of seismic sources as random and by introducing

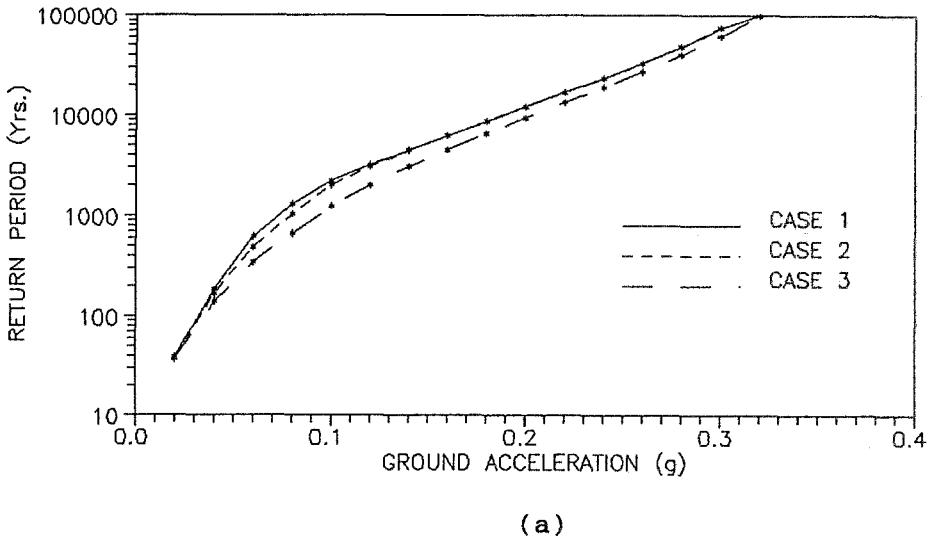

(a)

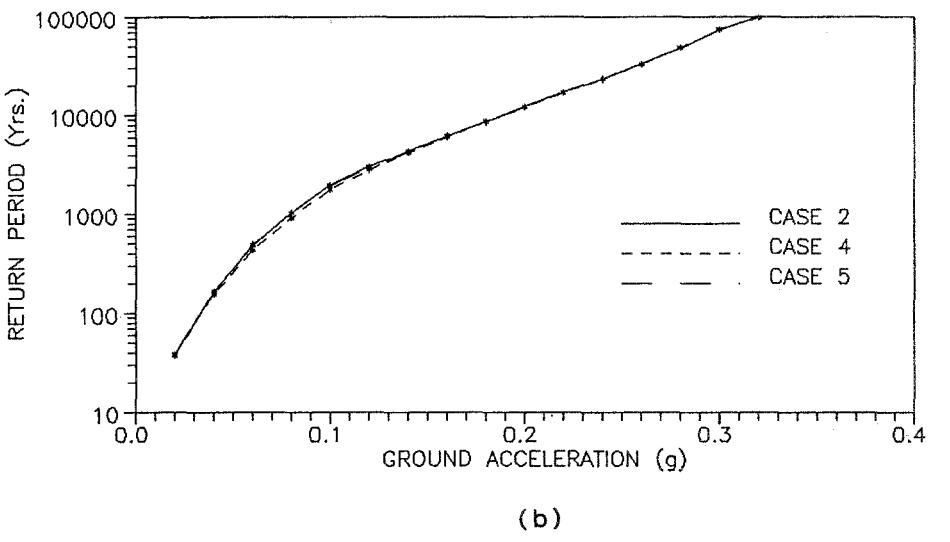

(b)

Fig. 11. Hazard calculated for the site shown in Figure 10.

measures of spatial variability in two orthogonal directions. Setting these measures of variability to zero reduces the model to the deterministic location case.

The two hypothetical case studies indicate that a biased location uncertainty in defining the source location can have a controlling effect on the level of calculated hazard at points situated close to these boundaries. Regardless of whether the uncertainty is isotropic or possesses a directional bias, it smooths the transition of the calculated hazard level for neighboring points belonging to different seismic regimes. This is in agreement with the simple heuristic argument that earthquake expectations at close distances should not exhibit abrupt variations because they have been assumed to belong to sources which nucleate radically different numbers of earthquakes. In actual cases involving a multitude of sources of either types, the randomness of the boundaries produces a great degree of smoothing, and influences the hazard estimate to a relatively smaller extent.

Acknowledgements

The Research Fund of Middle East Technical University under grants AFP 90-01-09-01, AFP 90-03-03-05 and 91-01-09-01 are gratefully acknowledged. We also thank graduate assistants Nesrin Basoz and Aysen Akkaya who did the numerical computations and the drawings.

References

Bender, B.: 1986, Modeling source zone boundary uncertainty in seismic hazard analysis, *Bull. Seism. Soc. Am.* **76** (2), 329–341.

Bender, B. and Perkins, D. M.: 1987, SEISRISK III: A computer program for seismic hazard estimation, USGS Bulletin 1772, Washington D.C., 48 pp.

Doyuran, V., Gulkan, P., and Kocyigit, A.: 1989, Seismotectonic evaluation of the Akkuyu nuclear power plant site, Report No. 89–01, Earthquake Engineering Research Center, Middle East Technical University, Ankara, 69 pp.

Gulkan, P. and Yucemen, M. S.: 1977, Seismic risk analysis for nuclear power plants, *METU J. Pure Appl. Sci.* **10**(1), 115–135.

Gulkan, P. and Yucemen, M. S.: 1991, Seismic hazard determination in regions having diffused boundaries, *Proc. 4th Intern. Conference on Seismic Zonation*, Vol. 2, Stanford, California, pp. 65–70.

McGuire, R. K.: 1976, Fortran computer program for seismic risk analysis, USGS Open-File report 76–67, 90 pp.

Slemmons, D. B.: 1977, State-of-the-art for assessing earthquake hazard in the United States, Part 6, faults and earthquake magnitude, U.S. Army Corps of Engineers, Vicksburg, 129 pp.

U.S. National Committee for the Decade for Natural Disaster Reduction: 1991, *A Safer Future: Reducing the Impacts of Natural Disasters*, National Academy Press, Washington, D.C.